Biophysical Chemistry 301 (2023) 107092

Contents lists available at ScienceDirect

Biophysical Chemistry

journal homepage: www.elsevier.com/locate/biophyschem

Direct interaction between the transmembrane helices stabilize cytochrome P450 2B4 and cytochrome b5 redox complex

Bikash R. Sahoo [*], Ayyalusamy Ramamoorthy [*,1]

Biophysics Program, Department of Chemistry, Macromolecular Science and Engineering, Biomedical Engineering, Michigan Neuroscience Institute, The University of Michigan, Ann Arbor, MI 48109-1055, USA

ARTICLE INFO

Keywords:
Cytochrome-P450
Cytochrome-b5
Redox complex
Lipid bilayer
Transmembrane-transmebrane
Structure

ABSTRACT

The catalytic activity of cytochrome P450 2B4 (CYP2B4) is moderated by its cognate redox partner cytochrome *b*5 (Cyt-b_5). The endoplasmic reticulum (ER) membrane and intermolecular transmembrane (TM) interaction between CYP2B4 and Cyt-b_5 regulate the substrate catalysis and the reaction rate. This emphasizes the significance of elucidating the molecular basis of CYP2B4 and Cyt-b_5 complexation in a membrane environment to better understand the enzymatic activity of CYP2B4. Our previous solid-state NMR studies revealed the membrane topology of the transmembrane domains of these proteins in the free and complex forms. Here, we show the cross-angle complex formation by the single-pass TM domains of CYP2B4 and Cyt-b_5, which is mainly driven by several salt-bridges (E2-R128, R21-D104 and K25-D104), using a multi-microsecond molecular dynamic simulation. Additionally, the leucine-zipper residues (L8, L12, L15, L18 and L19 from CYP2B4) and π-stacking between H23 and F20 residues of CYP2B4 and W110 of Cyt-b_5 are identified to stabilize the TM-TM complex in the ER membrane. The simulated tilts of the helices in the free and in the complex are in excellent agreement with solid-state NMR results. The TM-TM packing influences a higher order structural stability when compared to the complex formed by the truncated soluble domains of these two proteins. MM/PBSA based binding free energy estimates nearly 100-fold higher binding affinity (ΔG = -2810.68 ± 696.44 kJ/mol) between the soluble domains of the full-length CYP2B4 and Cyt-b_5 when embedded in lipid membrane as compared to the TM-domain-truncated soluble domains (ΔG = -27.406 ± 10.32 kJ/mol). The high-resolution full-length CYP2B4-Cyt-b_5 complex structure and its dynamics in a native ER membrane environment reported here could aid in the development of approaches to effectively modulate the drug-metabolism activity of CYP2B4.

1. Introduction

The microsomal cytochrome P450 monooxygenase (CYP450) enzymes [1] are a class of heme binding ubiquitous enzymes primary involved in the metabolism of xenobiotic compounds including endogenous and exogenous substrates such as lipids, steroids, environmental chemicals etc. [2–5] The topology of CYP450 share a single-pass transmembrane (TM) [6] helix anchored to the endoplasmic reticulum (ER) membrane and its catalytic activity is modulated by its redox partners through sequential electron transport. [7–9] Cytochrome-b5 (Cyt-b_5; secondary electron donor) [10] is a heme-protein characterized with a single-pass TM domain that synergistically work with cytochrome P450 reductase (CPR; primary electron donor) to regulate the activity of P450s. [11–14] CPR alone can modulate P450's activity by directly donating both electrons, while in some cases it is shown that the rate of kinetics is accelerated by ~10–100 folds in the presence of Cyt-b_5. [15] Notably, it is evidenced that the stoichiometry between Cyt-b_5 and CPR and their membrane environment plays a critical role on CYP450's catalytic activity. In addition, mutational studies on Cyt-b_5 shown a dramatic change in the rate of enzymatic kinetics of CYP450 in vivo. [16] The role of Cyt-b_5 in regulating the catalytic activity of CYP450 has been well-known in different organisms including human. [17] Recently reported NMR experiments showed the importance of membrane by probing the competitive interaction between P450 and its redox partners (b5 and CPR) in the presence and absence of lipid bilayer. [18,19]

It is important to decipher the role of structural interactions in the

* Corresponding authors.
E-mail addresses: bsahoo@umich.edu (B.R. Sahoo), ramamoor@umich.edu, aramamoorthy@fsu.edu (A. Ramamoorthy).
[1] Present Address: The National High Magnetic Field Laboratory, Department of Chemical and Biomedical Engineering, Florida State University, Tallahassee, FL 32310, United States.

https://doi.org/10.1016/j.bpc.2023.107092
Received 12 June 2023; Received in revised form 6 August 2023; Accepted 7 August 2023
Available online 8 August 2023

CYP450-Cyt-b_5 complex at an atomic level to better understand the mechanism of drug-metabolism. However, the lacuna in obtaining high-resolution structural information has been a roadblock to establish a structure-to-function relationship. In addition, the complexity of the system that involves all binding partners (CYP450, CPR and Cyt-b_5) localized in the endoplasmic reticulum (ER) membrane [20] limits structural interpretation. Previous studies have shown that the catalytic activity of CYP450 is strongly modulated by its membrane localization and membrane composition that facilitates the complex formation. [20–23] In addition, it is established that the TM helical domain of cytochrome P450 and b_5 is critical for its catalytic activity; however, the high-resolution structure and dynamics information are still not fully understood. The regulatory role of Cyt-b_5 on the catalytic efficacy of CYP450 enzyme is hypothesized to be regulated by its variable binding mode. [24] For example, NMR titration studies revealed different binding interface for Cyt-b_5 interacting with CYP2A6, CYP2E1 and CYP3A4 with affinities in the order CYP3A4 > CYP2A6 ~ CYP2D6 > CYP2E1. [24] Other studies have reported that Cyt-b_5 has a distinct effect on P450's substrate metabolism and P450's conformational states highlighting the complexity of the biochemical process. [25–27] What controls these biochemical process is still an open question, and a growing evidence suggests that the conformational linkage between P450 and its reducing partners and membrane could be important. [5,24] For example, the conformational states of CYP17A1 were shown to be influenced by Cyt-b_5. [25] Despite these recent advances in revealing the role of membrane and conformational dynamics in regulating P450's function, high-resolution details of this molecular processes remains to be explored. Thus, probing the structural interaction of full-length CYP450 with Cyt-b_5 proteins in a lipid membrane environment is highly important. Our research previously studied the structural interactions between the proteins, membrane topology, and electron-transfer pathway in the CYP2B4-Cyt-b_5 redox complex using a combination of solution and solid-state NMR experiments on membrane mimetic systems that includes bicelles (DLPC/DHPC) and nanodiscs (DMPC). [21,28,29] Recently, we reported the stability and structural folding of CYP2B4 modulated by the lipid composition and observed its preferential binding to sphingomyelin in the ER membrane mimetic nanodiscs. [22] These observations suggest that the structural interpretation of the dynamic interaction of CYP2B4 with Cyt-b_5 in ER membrane mimetic systems could provide additional valuable information to explore the catalytic mechanism of action of the CYP2B4 enzyme.

Although the membrane topology of the TM helices of Cyt-b5 and CYP2B4 has been determined by solid-state NMR spectroscopy of aligned lipid bilayer samples, [30–32] the membrane-bound redox complex system pose many challenges for atomic-resolution structural studies. One of the key challenges is in elucidating the structural information of the TM domain(s) and their role in (i) the redox complex formation, (ii) dynamic protein-protein and protein-lipid interactions, and (iii) the structural stability. It should be noted that, the activity of CYP2B4 has been shown to be stimulated by ~10 folds when it binds to Cyt-b_5 indicating structural rearrangement embedded in a membrane system. [33] To retrieve these structural and mechanistic insights at a molecular level, in this study we used multi-microsecond time-scale coarse-grained (CG) and nanosecond all-atom (AA) molecular dynamics (MD) simulations. MD simulations of P450 enzymes in a membrane environment (lipid-bilayer and nanodiscs) have revealed significant structural and mechanistic insight across different species and classes of cytochrome P450 enzymes. [34–38] Here, we used a multiresolution modeling strategy to build full-length CYP2B4-Cyt-b_5 complex embedded in ER lipid membrane and provided a structural and dynamic picture for TM-TM interactions that modulates the structure, dynamics, and stability of the CYP2B4-Cyt-b_5 complex.

2. Methods

Full-length structure building

The structures of the full-length CYP2B4 and Cyt-b_5 were built using an experimental-computational structure hybridization as we reported earlier. [22] Briefly, the crystal structures of the soluble domains of rabbit CYP2B4 (PDB ID: 1SUO) and Cyt-b_5 (PDB ID: 2M33) previously used to generate the CYP2B4-Cyt-b_5 complex were used for generating the full-length structures. The TM domain of both enzymes were constructed using ab-initio building by I-TASSER. [39] The model TM domains were concatenated with the experimental soluble domain structures using MODELLER v9.18 [40] and the HEME coordinates were copied. The CYP2B4-Cyt-b_5 complexes with and without the TM domains were built using default parameters in HADDOCK v2.2 [41] as detailed elsewhere inputting the NMR distance constraints. [42]

3. MD simulations

3.1. All-atom MD simulation

MD simulation of the full-length or the TM-domains-truncated complex was performed in GROMACS 5.0.7 running parallel on an SGI UV-3000 system. The 3D coordinates of ER membrane composed of a total number of 205 lipids POPC/POPS/POPE/POPI/PSM/Cholesterol (58/7/20/7/4/4%) was built using CHARMM-GUI. [43] The pre-equilibrated ER membrane was simulated for 50 ns to optimize the bilayer organization prior to membrane protein insertion. The protocol for the construction of the CYP2B4-Cyt-b_5 complex embedded in ER membrane was adopted from our previous study. [22] The complex structure was oriented in the ER membrane using the *g_membed* program followed by solvation using TIP3 water model. The axis parallel to the bilayer normal was extended to add more water molecules to adequately embed the cytoplasmic (or the soluble heme-containing) domains of CYP2B4 and Cyt-b_5. The TM truncated soluble domain complex structure of CYP2B4-Cyt-b_5 was solvated using a cubic box of dimension 11 × 11 × 11 nm^3. Both full-length and truncated complex structures were neutralized by adding counter ions, and a salt concentration of 0.1 M was used for simulation using Charmm36-ff. [44] The MD systems were energy minimized using the steepest descent method followed by equilibration using a short NVT of 0.2 ns or 5 ns NPT simulation. The parameters of MD simulation such as non-bonded interaction cutoff, long-range and short-range interactions were adopted as described elsewhere. [45] MD simulation of the redox complex in ER membrane was performed at 303.15 K for proteins and water, whereas 315.15 K was used for the ER membrane that allows the system to simulate above the phase transition temperature of mixed lipids. MD simulation for the truncated soluble protein-protein complex was carried out at 303.15 K. A final production MD run of 100 ns was executed for each MD complex system. The MD trajectory of the complex obtained from 100 ns MD calculation is analyzed using in-house GROMACS commands and visual molecular dynamics (VMD) program. Protein structure visualization was carried out using VMD, discovery studio visualizer (DSV v3.5), PyMOL v4.6 (https://pymol.org/2/) and Chimera v1.14. [46] Statistical analysis and plots were generated using Origin 2019 (9.6.0.172). The protein-protein residue specific interaction sites and bond information were generated using DSV and LigPlot$^+$. [47]

3.2. CG MD simulation

The CG MD simulation of the full-length CYP2B4-Cyt-b_5 complex was performed under an identical condition (MD simulation parameters) in ER membrane. The protein-membrane system was built using CHARMM-GUI [43] using ER lipid composition identical to our all-atom MD simulation. Martini v.2.2 force field [48] was used for the protein and v2.0 for lipid and ions MD simulation. The membrane temperature was maintained above the main phase transition temperature of lipids

(315.5 K) to represent the lamellar phase of the lipids. Short NVT (0.5 ns) and long NPT (1 μs) simulation were carried out to equilibrate the MD systems. A final production MD run of 11.4 μs was carried out using 0.02 ps time-step for integration. The MD trajectory was analyzed using GROMACS and VMD. The CG coordinates obtained from 11.4 μs MD simulation were back converted to all-atom coordinates for the complex structure analysis using DSV and Chimera.

3.3. MM/PBSA binding free energy calculation

The binding free energy between the CYP2B4 and Cyt-b_5 in the redox complex was estimated using MM/PBSA method which has been previously tested on protein-protein [45] as described elsewhere. [49,50] Using an integrated GROMACS and APBS (GMXPBSA) [51,52] commands, the energetic parameters are computed from 100 different snapshots retrieved at a regular time interval from the 100 ns MD simulation. For a comparative analysis, CYP2B4 coordinates consisting of amino acids 51–492 and Cyt-b_5 residues 1–90 (the soluble domains) were retrieved from full-length and TM domain truncated complexes by creating specific index files. The lipid, TM domain, and unstructured linker residues were not considered for MM/PBSA computation.

4. Results and discussion

4.1. Orientation of TM helices in the CYP2B4-Cyt-b_5 complex in ER membrane

The full-length structures of the CYP2B4 and Cyt-b_5 were generated by structural hybridization of experimental and ab-initio model structure of the soluble and TM domain, respectively. The CYP2B4-Cyt-b_5 complex was built using HADDOCK web-program guided with the NMR distance constraints. [42] The initial complex structure was stabilized by salt-bridges, hydrogen bonds and alkyl interactions. We note that in CYP2B4 the R125 forms a hydrogen bond with heme-D-propionate, whereas the R126's sidechain is exposed to the protein-protein interface in the redox complex (Fig. S1). This is well supported by the importance of R125 in the electron transfer between cytb5 and cytP450 revealed by our previous experimental study. [42] The stability of the full-length CYP2B4-Cyt-b_5 complex was first studied using coarse-grained (CG) MD simulation on a timescale of 11.4 μs by incorporating the TM helices in a lipid-bilayer that mimics the lipid composition of ER membrane. As shown in Fig. 1a, TM domains of the initial complex structure in our CG-MD were separated by at least >2 nm inside the ER membrane before the MD simulations. The TM-TM interaction and its effect on the complex structure are revealed at the end of 11.4 μs MD simulation. The TM-TM interaction rearranges the helices with a cross-angle structure where each helix is oriented ~10°-20° with respect to bilayer normal (Fig. 1b), which is in agreement with previous solid-state NMR experimental studies. [29] The TM-TM interaction is shown to influence the interaction between the soluble domains of CYP2B4 and Cyt-b_5 highlighting a tight binding as illustrated in Fig. 1b. The formation of a tight complex induced by the TM-TM interaction is preceded by several intermediate conformations where both the proteins show substantial TM helix dynamics and tilt (Fig. 2).

Structural analysis of the complex derived from CG-MD as a function of simulation time as shown in Fig. 2 revealed a slow and flexible TM helix rearrangement in both proteins prior to the TM-TM crossing. During the initial 0.6 μs, a substantial structural rearrangement is noticed on the soluble domain of Cyt-b_5. A translational shift of ~8 Å (away from CYP2B4 TM helix) is observed for the residue located at the center of the Cyt-b_5-TM helix from its initial position ($t = 0$ μs); whereas the C-terminal residues (Asp133 and Asp134) showed an inward movement (towards CYP2B4 TM helix) (Fig. 2a, red and green). This structural rearrangement in the TM domain is found to be flexible during the next 2.4 μs showing both inward and outward translational movement with respect to the bilayer normal. Notably, the TM domain translation facilitates the Cyt-b_5 soluble domain with an increase in the intermolecular contact surface area as illustrated in Fig. 2a (red versus purple). A considerable downward (towards bilayer surface) movement of the Cyt-b_5 soluble domain is identified resulting in a displacement of 20.2 Å between the N-terminal methionine before and after 2.4 μs MD simulations (Figs. 1a and S1a). The resulting displacement of Cyt-b_5

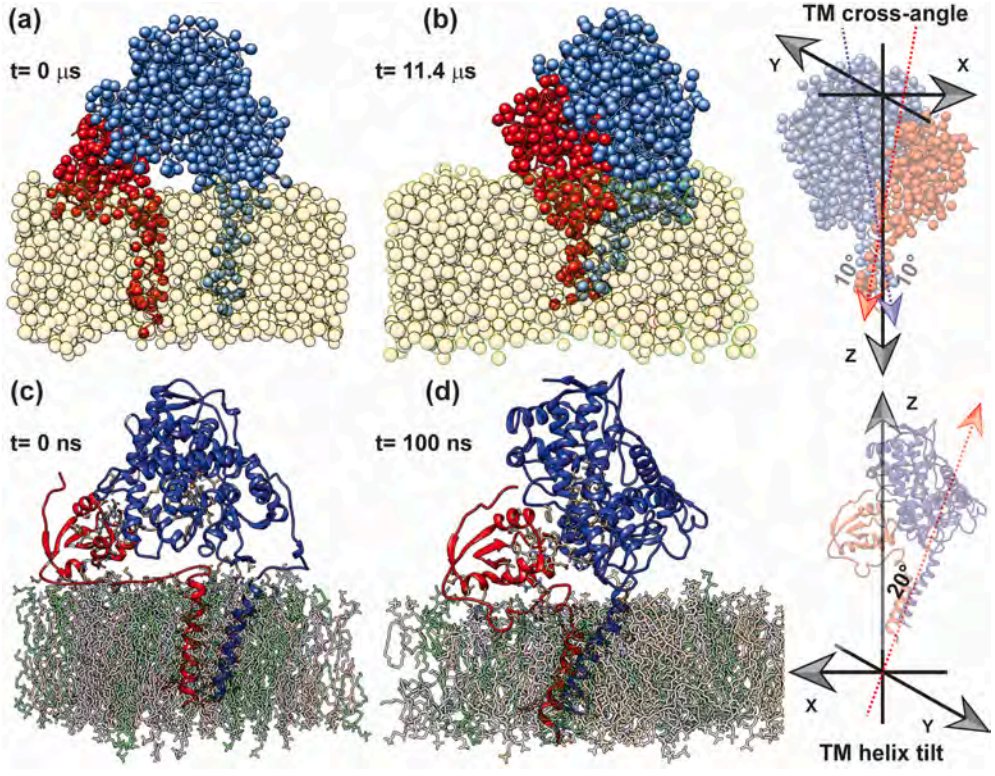

Fig. 1. Structure, dynamics, and orientation analysis of full-length CYP2B4-Cyt-$b_5$complex in ER membrane. (a) The initial coordinates (time = 0 μs) of the CG model structure of the CYP2B4-Cyt-b_5 complex in ER membrane, and MD snapshots of the final structure retrieved at 11.4 μs (b). CYP2B4, Cyt-b_5, and lipid-bilayer are respectively shown in blue, red and yellow and represented in spheres. A schematic is drawn to illustrate the TM-TM cross-angle (denoted as dotted arrows) conformation as derived from the final structure shown in (b). The all-atom model structure of an intermediate CYP2B4-Cyt-b_5 complex embedded in the ER membrane is shown at time = 0 ns (c) and time = 100 ns (d). The protein is shown as cartoon (blue: CYP2B4, red: Cyt-b_5) and lipid as sticks. The TM helix tilt as derived from (d) is shown on the right as indicated by a dotted arrow. The cross- and tilt-angles for the TM domains are calculated with respect to the bilayer normal.

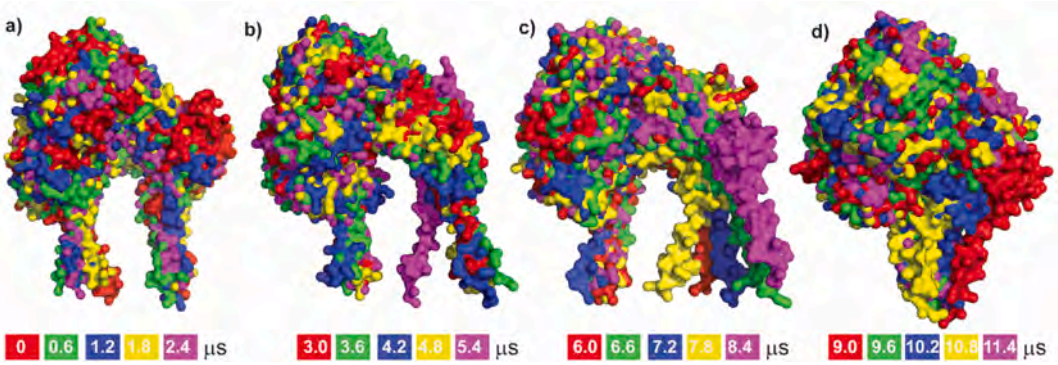

Fig. 2. Conformational changes in CYP2B4-Cyt-b$_5$complex as a function of time. CG-MD snapshots show the structural dynamics of TM domains retrieved at a variable time-points as indicated in colors. Five representative structures of the CYP2B4-Cyt-b$_5$ complex derived at a time-interval of 0.6 μs (a-d) as indicated are superimposed where CYP2B4 structures are presented on the left and Cyt-b$_5$ on the right from the complex center in each superimposed structure.

soluble domain assists electrostatic interaction between R120, R122 and R126 from CYP2B4 and E42, E43, E48 and E49 from Cyt-b5 (Fig. S1b). The complex stability is identified to be highly transient in the next 6 μs (2.4–8.4 μs) MD simulations where the Cyt-b$_5$ TM domain majorly rearranged in the lipid bilayer generating a loose or tightly bound protein-protein complex structure (Fig. 2). At 5.4 μs both TM domains were identified to be oriented at a close proximity for association following dissociation at 8.4 μs (Fig. 2b and c). The association and dissociation of the TM domains is reciprocated by the soluble domain electrostatic interactions as highlighted in Fig. S1b. Interestingly, a stable complex is formed from 9 μs to 11.4 μs modulated by the TM-TM interaction. The initial TM-TM helix interaction is driven by a salt-bridge involving Glu2 (CYP2B4) and Arg126 (Cyt-b$_5$) following leucine zipper packing (Figs. 2d and S2). The spontaneous assembly of TM-TM helices has been previously observed for CYP1A2 and Cyt-b$_5$ by MD simulation driven by the flexible linker interaction embedded in a simplified DLPC membrane. [38] However, we do not see any interaction between linkers in the CYP2B4-Cyt-b$_5$ complex, and found the soluble domain rearrangement drives the TM-TM interaction or vice-versa in both CG and all-atom MD simulations. This could be due to the effect of membrane composition; unlike DLPC that forms a thin bilayer with a hydrocarbon thickness of 21.9 Å, [53,54] the ER membrane is thick with a hydrocarbon thickness > 30 Å, [22,54] ordered and forms lipid rafts that constrain the dynamics of embedded protein. The native membrane environment is proposed to be important to fully capture the functional state of membrane proteins. Notably, MD simulation that presented a cross-angle TM helix orientation for CYP2B4-Cyt-b$_5$ complex has also been observed for CYP1A2-Cyt-b$_5$ complex with a relatively high TM helix tilt with respect to the lipid bilayer normal [38], and in agreement with solid-state NMR findings. [55] Collectively, this observation hints the cross-angle orientation of TM helices may influence the functional role of CYP2B4 in its native state.

4.2. Atomistic insights into TM-TM helix interactions in the CYP2B4-Cyt-b$_5$ complex

To further gain insight into the early stage of TM-TM interactions at an atomic level, we next performed all-atom MD simulations that are limited by the united-atom model system shown in Fig. 2. In our all-atom MD simulations, to reduce the timescale of TM-TM interactions (within nanoseconds) as revealed from our united model CG-MD calculation, the TM helices were initially separated by a minimum distance ~1.0 nm (Fig. 1c) that resembles the complex structure obtained from CG-MD at a timescale of 7.8 μs. The simulated CYP2B4-Cyt-b$_5$ complex embedded in the ER membrane showed TM-TM interaction within the chosen 100 ns time-scale as illustrated in Fig. 1d. Remarkably, a TM helix tilt ~10°-20° was observed for the TM-TM domain complex with respect to the ER membrane normal and also reported previously for model structures of CYP450 in lipid-bilayer [56] and by solid-state NMR experiments on a fluid lipid bilayer. [55] In addition, the TM helix tilt in the CYP2B4-Cyt-b$_5$ complex resemble the intermediate structures obtained from our CG-MD results that show a gradual increase in TM-TM packing arbitrated by the leucine-zipper sequence in the TM helices. We do not observe a cross-angle TM-TM orientation from our all-atom MD simulation within the timescale of 100 ns. This agrees with the CG-MD results that indicate a transition from an open tilted (Fig. S2, left) to a cross-angle TM orientation (Fig. S2, right) requires hundreds of nanoseconds. A notable observation from all-atom MD simulation is the relative orientation of the TM helices. As shown in Fig. S3, a two-turn helix offset is observed for Cyt-b$_5$ TM allowing a spatial orientation for the salt-bridge formation (Glu2-Arg128).

The atomic interaction map of the CYP2B4-Cyt-b$_5$ complex was next analyzed from all-atom and MD simulations. The intermediate complex structure as obtained from 100 ns all-atom MD simulation shows both electrostatic and hydrophobic packing as illustrated in Fig. 3. The TM-TM complex stabilized by the Glu2-Arg128, Arg21-Asp104 and Lys25-Asp104 salt-bridges is reciprocated by hydrophobic packing across the leucine zipper (Figs. 3a, c and 4). Electrostatic potential map shows a close contact between the acidic (Glu2) and basic (Arg128) surface in CYP2B4 and Cyt-b$_5$, respectively (Fig. 3c). A similar electrostatic surface potential is observed in the TM-TM complex structure obtained from CG-MD simulation. We note that the surface potential was calculated using an all-atom TM-TM complex obtained by back converting the CG coordinates. Notably, in the all-atom intermediate TM-TM complex, the C- and N-termini of CYP2B4 and Cyt-b$_5$, respectively, do not show any interactions (Fig. 3c). However, these regions are identified to interact on a long-time scale CG-MD simulations (Fig. 3d). In addition to the E2-R128 salt-bridge as observed in the intermediate structure (Fig. 3c and e), additional salt-bridges were identified at R21-D104 and K25-D104 in CG-MD simulations (Figs. 3d, f and 4). The leucine-rich region ^{5}**LLLLLAFLAGLLLLL**^{19} in CYP2B4 showed hydrophobic packing with the Cyt-b$_5$ region spanning residues ^{114}VIPAISALIVALM^{126}. CYP2B4 leucine residues that include Leu8, Leu12, Leu15, Leu18 and Leu19 were found form hydrophobic packing with Cytb$_5$ enzymes Ala124, Arg128, Leu121, Ala120, Tpr109, Trp110, Trp113 and Ala117 (Fig. 4). Our simulation results are in agreement with our previous solid-state NMR observations that showed the involvement of Leu121 and Leu125 residues in intermolecular interactions in a lipid bilayer. [55] We note that Fig. 4 is a representative interaction plot derived at the end of 11.4 μs, and we see the involvement of Leu125 in hydrophobic packing in our MD simulation at different time-points (data not shown). In addition to hydrophobic packing, the Trp110 in Cyt-b$_5$ shows π-stacking interaction with CYP2B4's His23 and Phe20 (Fig. 4). Together, the MD simulation provides an atomistic detail for the residues driving TM-TM interaction that were incomplete in our previous NMR study [55] due to selective ^{13}C labeling and experimental challenges.

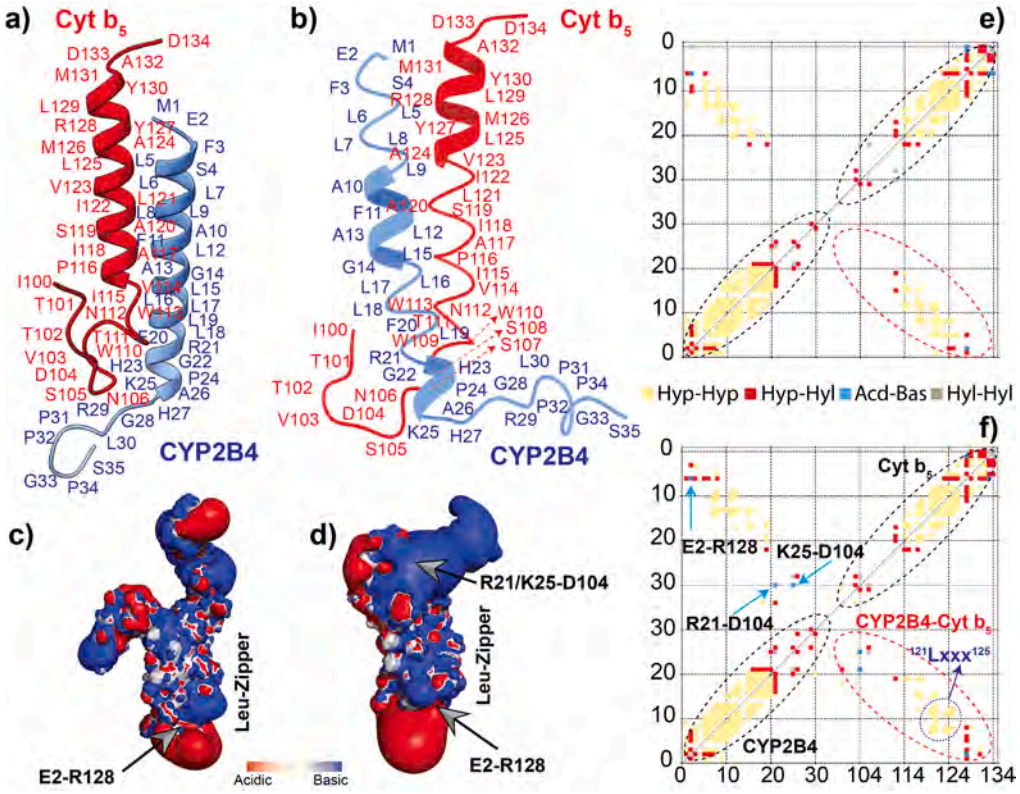

Fig. 3. Structural interactions between the TM domains of CYP2B4 and Cyt-b_5. Snapshots of CYP2B4-Cyt-b_5 complex retrieved from 100 ns all-atom (Cyt-b_5 residues are not labelled) (a), and 11 μs coarse-grained (b) MD simulations embedded in ER membrane (shown as dots). Zoom in atomistic interactions between TM-TM domain obtained from all-atom (c), and coarse-grained MD (d) at the indicated color. The coarse-grained TM coordinates shown in (d) are back converted to all-atoms and amino acids are labelled. Contact map analysis of TM-TM interactions obtained from all-atom (e) and coarse-grained (f) MD simulations. The intra- and inter-molecular interactions are shown inside dotted red and black circles, respectively. We note the intermolecular interactions are a mirror image of each other. The intermolecular salt-bridges are shown in light-blue arrows and leucine-zipper packing in dark-blue arrows. (For interpretation of the references to color in this figure legend, the reader is referred to the web version of this article.)

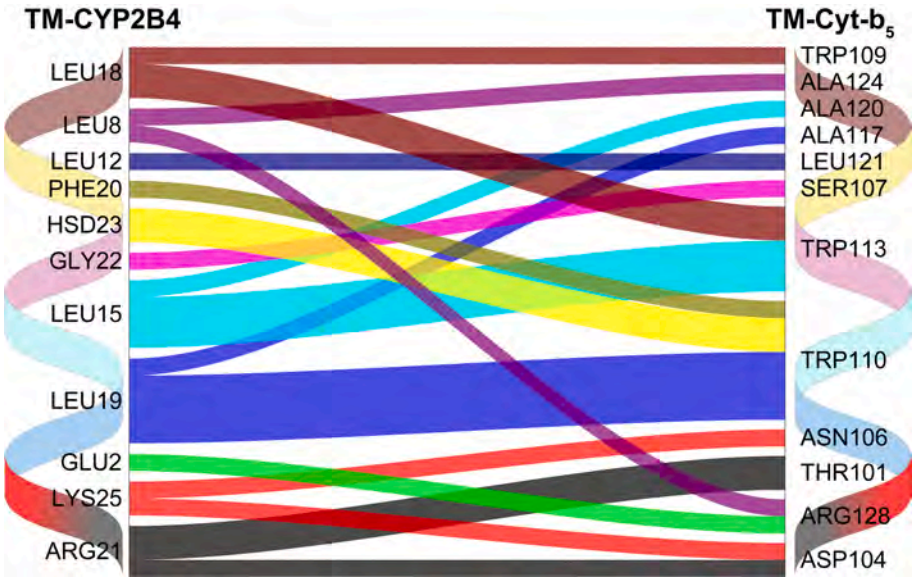

Fig. 4. Residue specific interaction plot of TM-TM domains retrieved from 11.4 μs CG-MD simulations. Residues involved in salt-bridge (attractive) interactions are GLU2, LYS25 and ARG21 (from CYP2B4) and ARG128 and ASP104 (from Cyt-b5), and residues involved in π-stacking are PHE20 and HIS23 (from CYP2B4) and TRP110 (from Cytb5). Leucine zipper residues (L8, L12, L15, L18 and L19) are involved in hydrophobic packing as indicated. The line thickness corresponds to the interaction strength; for example, the top most line thickness is for a single bond interaction.

4.3. TM-TM interaction stabilizes CYP2B4-Cyt-b_5 complex

To understand the influence of TM-TM interaction on the structural interaction between the soluble domains in CYP2B4-Cyt-b_5 complex, we next performed MD simulation of truncated (tr) CYP2B4-Cyt-b_5 complex (with no TM domains). Analysis of the protein backbone root mean square deviation (RMSD) derived from 100 ns all-atom MD simulation of the full-length CYP2B4-Cyt-b_5 complex showed a high RMSD values for the Cyt-b_5 (Fig. 5a, green vs red) when compared to the truncated CYP2B4-Cyt-b_5 complex (100 ns). On the other hand, no significant change (Fig. 5a, blue vs black) in RMSD is observed for the CYP2B4 indicating the structural rearrangement is majorly contributed by the Cyt-b_5 in the hetero-complex. Similarly, RMSD of Cyt-b_5 TM helix was found to be higher as compared to that of CYP2B4 further supporting both soluble and TM domain of Cyt-b_5 mediates hetero-complex formation. We note that the reported observations could be due to the absence of P450 substrate; and in the presence of substrate the protein dynamics may be different. The increase in structural flexibility in Cyt-b_5 not only affects the soluble domain's interaction, but also influences the orientation of TM-TM helices in the ER membrane. CYP2B4's rigidity and Cyt-b_5's flexibility may facilitate a topology that is required for the catalysis of substrate and recruiting other binding partners such

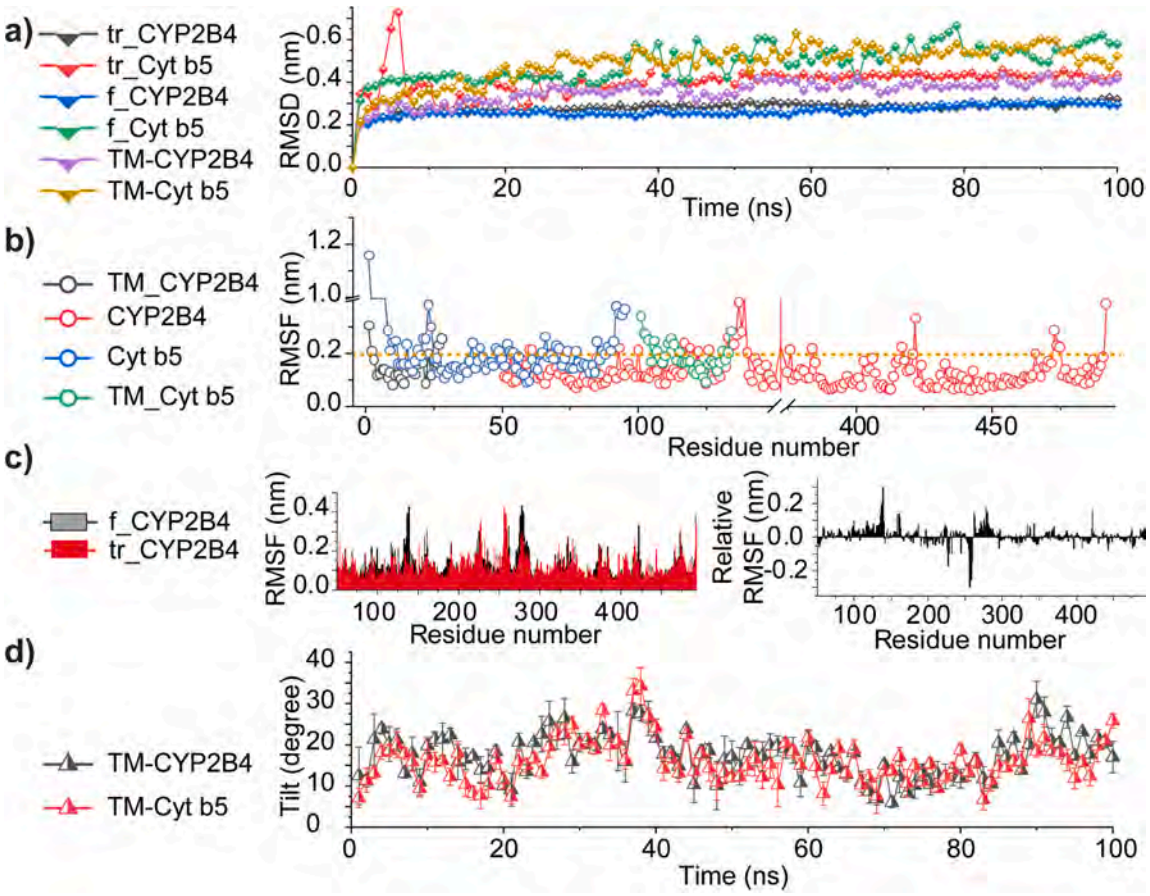

Fig. 5. Comparative structural dynamics and stability analysis between the full-length and truncated (tr) CYP2B4-Cyt-$b_5$complexes. (a) The RMSD profile analysis of different functional domains in CYP2B4-Cyt-b_5 complex as indicated in colors calculated from 100 ns all-atom MD simulations. The truncated and full-length protein complex respectively are denoted with a prefix "f_" and "tr_". (b) The RMSF graph calculated for individual domains from the CYP2B4-Cyt-b_5 complex are shown as a function of residue number. The dotted line shows a RMSF value over 2 Å. (c) The RMSF profiles of soluble domains in the full-length and truncated CYP2B4-Cyt-b_5 complexes are compared and the relative RMSF (with respect to the full-length complex) is plotted on the right. (d) The tilt-angles in TM domains calculated from the CYP2B4-Cyt-b_5 complex with respect to the parallel oriented ER membrane surface as a function of time. All the profiles shown here (a-d) are calculated from 100 ns all-atom MD simulations and indicated with colors as shown on the left panel.

as CPR.

The root mean square fluctuation (RMSF) calculated as a function of amino acids showed a high fluctuation both in the truncated and full-length Cyt-b_5 N-terminus that share a random-coil structure (Figs. 5b (blue) and S4 (black and red)). The RMSF values calculated for the TM domain of Cyt-b_5 is comparatively higher than for CYP2B4-TM domain (Fig. 5b, green vs black) that shows a RMSF value <2 Å for the TM helix (residues 3–24). This observation correlates the notable dynamic behavior of Cyt-b_5 TM domain in mediating the TM-TM interaction as illustrated in Fig. 2. The relative RMSF values of CYP2B4 in the TM-truncated complex were calculated in reference to the full-length CYP2B4-Cyt-b_5 complex. The RMSF plots showed a higher fluctuation in the C—D loop region (> 2 Å) spanning residues 137–140 that was identified in the proximity of the CYP2B4-Cyt-b_5 interface in the full-length protein-protein complex. In addition, loop fluctuations are observed for D-E (159–163), G-H (253–264) and H—I (277–281) loop residues. Interestingly, the R422 is the only residue in the CYP2B4 C-terminus that shows a considerable fluctuation and previously been identified as a key residue for Cyt-b_5 complex formation and drug-metabolism. [57] On the contrary, these fluctuations in the truncated soluble domain complex are comparatively small with exception to the G-H loop residues (257–260). Quantitative measurement of the TM helix tilt as illustrated in Figs. 1 and 2 as a function of time showed an average tilt of 15.5 ± 5.6° for the Cyt-b_5 TM helix, and 18.06 ± 5.7° for the CYP2B4 TM domain (Fig. 5d). Interestingly, the observed TM-TM orientation closely resembles a model structure constructed using solid-state NMR experimental constraints, [30] and the tilt angle matches well with the simulated tilt angle of Cyt-b_5 in DMPC/DHPC bicelles in free (14 ± 3°) and (16 ± 3°) complex state. [29] Recently, the helix tilt is shown to be influenced by force-field parameters, but notably a similar range of helix tilt (~10–20°) is observed for other class of CYPs. [58]

4.4. TM-TM interaction enhance cytoplasmic domain stability in CYP2B4-Cyt-b_5 complex

The interaction between TM domains was next studied to understand its influence on the structural stability of the complex. The physical and chemical properties of membrane and substrate binding are known to module the complex formation and stability of structural interactions between CYP2B4 and Cyt-b_5. [59,60] In our all-atom MD simulations, both CYP2B4 and Cyt-b_5 TM helices are observed to render an ideal helix conformation with a helicity over 80% for most of the residues in CYP2B4 (3−21) and Cyt-b_5 (114–130). We observed a secondary structure change in the TM domain of Cyt-b_5 that initially modeled with a longer helix (109–132) (Fig. S5). Notably, the ideal TM helix observed in Cyt-b_5 in our MD simulation correlates to the secondary structure determined by solid-state NMR using selective residue ^{13}C labeling. [30] Next, we compared the effect of the conformational alteration in the TM helix and in the TM-TM complex formation on the conformation of the

soluble-domains. The complex of the soluble domains of CYP2B4-Cyt-b_5 in the absence of TM domains and ER membrane shows a smaller number of hydrogen-bond contacts (Fig. 6b). On the other hand, the full-length proteins embedded in the ER membrane show a tight packing with a relatively high number of hydrogen bonds between the soluble domains as shown in Fig. 6c. The B- and D-helices, and loop connecting A'-B and C—D helices in Cyt-b_5 are found to contribute several hydrogen bonds and electrostatic interactions with CYP2B4.

Atomistic interaction analysis between the soluble domains of CYP2B4 and Cyt-b_5 in the presence of TM domains shows electrostatic interactions between the basic residues of CYP2B4 and acidic residues of Cyt-b_5. CYP2B4 residues R126, R133, and R262 were found to electrostatically interact with Cyt-b_5 residues E43, E48, E49, and D71 (Fig. 6d). Multiple hydrogen bonds are observed between these acidic and basic residues as illustrated by dotted lines in Fig. 6d. In addition, an electrostatic interaction between Cyt-b_5 N-terminal residue M1 and CYP2B4 D134 is also observed. Other residues that include CYP2B4 A130, G136, M137, and G138 were found to form hydrogen or hydrophobic packing with Cyt-b_5. These observations are in good agreement with the complex structure determined by NMR experiments of the full-length proteins in bicelles. [42] The perpendicularly oriented heme in Cyt-b5 with respect to CYP2B4's heme showed a substantial translation ~7.2 Å from its original position post 100 ns MD simulation (Fig. S6). The structural arrangement allowed the heme edges in the CYP2B4-Cytb$_5$ complex to come closer within the upper limit (~14 Å) for an efficient electron transfer. We note that a longer all-atom simulation may further refine the spatial arrangement of heme in the complex for an efficient electron transfer.

We compared the atomistic interaction map of CYP2B4-Cyt-b_5 complex obtained from our all-atom MD simulation with the final structure retrieved ($t = 11.4$ μs) from our CG-MD. Interestingly, several intermolecular contacts that were not observed in our 100 ns time-scale structural sampling are observed in the CG-MD simulations (Fig. 7). The N-terminal arginine residues R126, R133 and D134 in CYP2B4 were found to interact electrostatically with Cyt-b_5 E43, E48, and K39 respectively, where the residue E43 interacts with both R126 and R133. In addition, the acidic residues E43 and E48 were found to be involved in forming several hydrogen bonds as illustrated in Fig. 7. As compared to other residues, we observed R133 (CYP2B4) and E43 (Cyt-b_5) to be involved in multiple interactions that include electrostatic, hydrogen-bond and π-alkyl hydrophobic packing. Several C-terminal basic residues in CYP2B4 that include R271, K274, and K276 were also identified to mediate charge-charge interactions with D65, E61 and D58 (Cyt-b_5) residues, respectively. Notably, the E43 residue involved in multiple interactions with R133, was also found to interact with the C-terminal residues N423 and R434 in CYP2B4 highlighting its crucial role in the complex formation (Fig. 7). Other charged residues in CYP2B4 such as E86, E119, R271, D275, K276, and D278 are found to interact with W109, N106, D65, N62, G56 and R52 (Fig. S7). It should be noted that several of the interacting residues including R133 identified in our MD

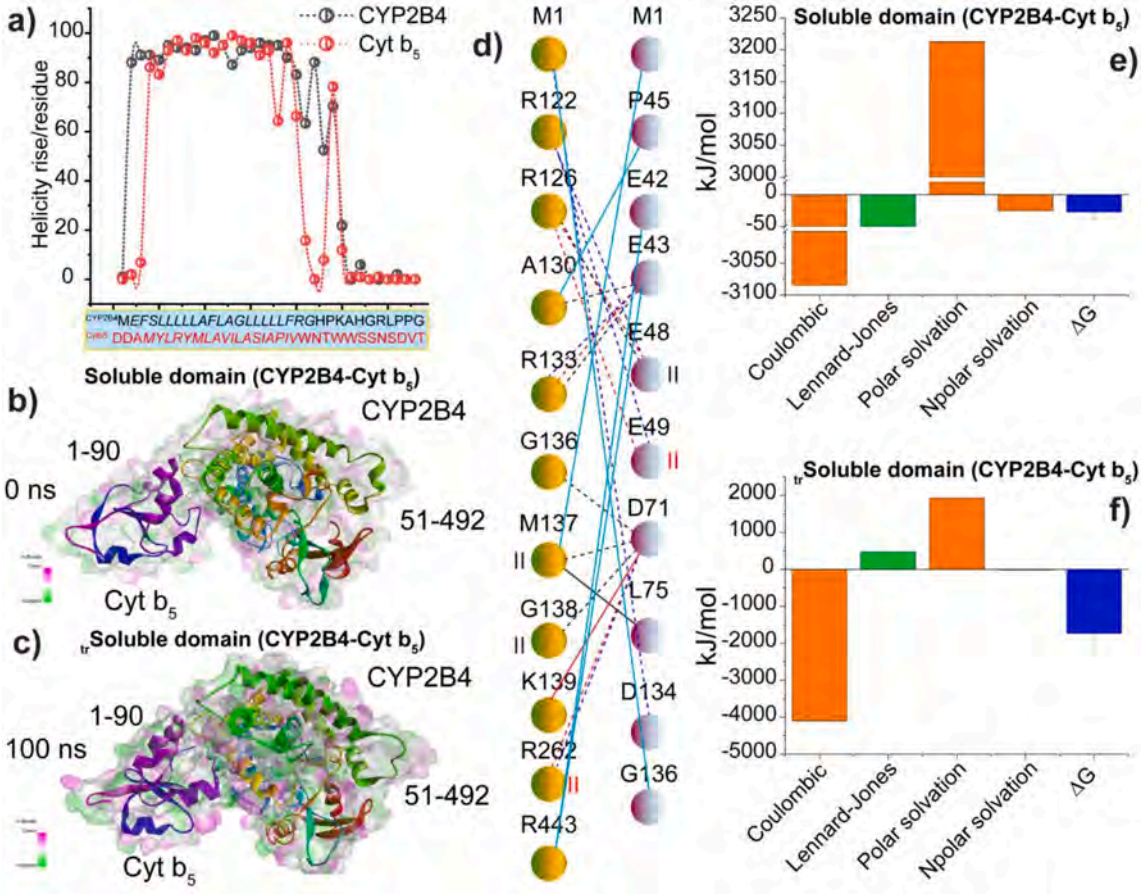

Fig. 6. Comparative atomistic interaction map and binding energetics between CYP2B4 and Cyt-b_5 in the presence and absence of membrane. (a) Secondary structure change in the TM helix as a function of residues obtained from 100 ns MD simulations. (b-c) Cartoon structure showing the soluble domain complex of CYP2B4-Cyt-b5 obtained from all-atom MD simulation of the soluble domain without TM (b), and the full-length protein in ER denoted as $_{tr}$Soluble domain (c). (d) The interaction map obtained from all-atom MD simulation representing an intermediate state of the CYP2B4-Cyt-b5 complex identifies several new contacts (dotted line) as compared to the soluble domain complex (solid line) without TM and membrane. The roman numbers indicate the number of hydrogen-bonds between two residues. (e-f) MM/PBSA based binding free energy and other energetic parameters computed from the CYP2B4-Cyt-b_5 complex in the absence (e) or presence of TM and membrane (f).

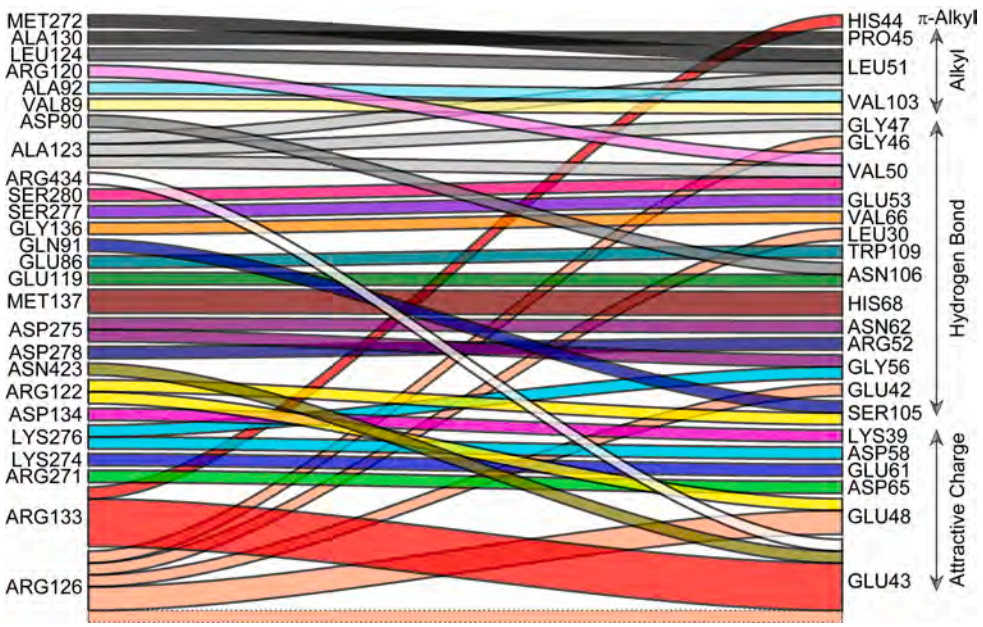

Fig. 7. Intermolecular interaction plot for the CYP2B4-Cyt-b_5 complex obtained from the CG MD snapshot retrieved at time 11.4 μs. The types of interaction between two residues are indicated on the right. The line thickness corresponds to the interaction strength, and the line thickness for a single bond interaction is shown inside a dashed box at the bottom. The line thickness corresponds to the interaction strength; for example, the bottom most line thickness is for a single bond interaction.

simulation have been shown to significantly change the binding affinity between CYP2B4 and Cyt-b_5 upon mutation as tested experimentally. [42]

The stability of the CYP2B4-Cyt-b_5 complex was next probed by computing the binding free energy using MM/PBSA. The different energetic parameters obtained from MM/PBSA calculations are plotted in Fig. 6e and f. The soluble domain of CYP2B4-Cyt-b_5 complex formation was found to be favored by both bonded and non-bonded (Coulombic and Lennar-Jones (L-J)) interactions. The interaction is highly disfavored by the polar solvation energy (3212.71 ± 543.76 kJ/mol) and countered by a small non-polar solvation energy (−25.39 ± 4.70 kJ/mol). The free binding energy (ΔG) computed for the soluble-domain complex in the absence of TM domains and membrane is ΔG = -27.406 ± 10.32 kJ/mol (Fig. 6f). Notably, a hundred-fold higher (ΔG = -2810.68 ± 696.44 kJ/mol) binding energy was computed for the soluble domains retrieved from the full-length CYP2B4-Cyt-b_5 complex (Fig. 6f). It should be noted that the estimated binding energy is not contributed from the TM-TM and membrane lipid intermolecular and intramolecular interactions (see methods). The MM/PBSA calculations in both systems do not consider the energetic parameters contributed from entropic calculations. However, the estimated binding energy for the soluble domains (ΔG = -27.406 ± 10.32 kJ/mol) closely equals the range of the experimentally calculated binding energy ΔG = -38.20 kJ/mol. It should be noted that the ΔG computed for the soluble domains extracted from the full-length complex cannot be calculated using experimental methods and thus cannot be compared. Assuming the reliability of the applied method on these systems under identical conditions, the computed ΔG values indicate TM-TM interaction and ER membrane incorporation influence the stability of the soluble domains of CYP2B4-Cyt-b_5 complex. The influence of lipid membrane and TM domains in modulating the protein-protein complex stability has previously been observed for several other proteins, [45,61–63] which further supports our distinguished observation of a higher ΔG for the CYP2B4-Cyt-b_5 complex in ER membrane.

The effect of membrane on P450 function is beyond triggering its complex formation with Cyt-b_5 as observed here. For example, the CYP2B4–Cytb_5 complex stability in a membrane environment could be eased by other P450 reductases such as CPR as demonstrated earlier. [19] In contrast, P450 substrate binding favors the stability of the CYP2B4-Cytb_5 by masking CPR. We believe that structural and dynamic studies of the ternary complex in a native membrane environment is crucial considering the dynamic exchange between CPR and Cytb_5 in binding to P450. However, a deeper understanding of this molecular process through a detailed structural and dynamic studies of the ternary complex would be essential.

5. Conclusion

A multiresolution structure of CYP2B4 and its interaction with Cyt-b_5 in a near natural membrane environment (ER membrane) is obtained using long-range MD simulation. Structural and dynamic analysis of the CYP2B4-Cyt-b_5 complex in the ER membrane identified a spontaneous and stable TM-TM domain interaction driven by salt-bridges, π-stacking, and leucine-zipper packing. Notably, the TM-TM interaction is shown to stabilize the soluble catalytic domain complex with a nearly hundred-fold higher binding affinity when compared with the CYP2B4-Cyt-b_5 complex that lacks a TM domain. The reported results that include residue interaction plot, TM helix tilt and dynamics are in good agreement with published experimental results; but provides a complete picture of the high-resolution structure and dynamic information of the CYP2B4-Cyt-b_5 complex embedded in ER membrane. Further structural studies probing the effects of lipid composition on the CYP2B4-Cyt-b_5 complex would be useful as a recent nanodiscs based NMR study [22] revealed the lipids preferred by CYP2B4, Cyt-b_5 and CPR. We expect the reported multiresolution model structure of the full-length CYP2B4-Cyt-b_5 complex in a native ER membrane system to be valuable in understanding the enzymatic function of cytP450s and could help understanding the mechanism of providing a high affinity drug metabolism. The reported structure could be utilized to devise experimental measurements towards understanding the role of a possible hydrophobic channel to enable the metabolism of hydrophobic compounds by P450s.

Author statement

B.S. and A.R. planned the research. B. S. carried out the simulations and analyzed the data. B. S. and A. R. interpreted the results and wrote the manuscript. Both read and approved the manuscript. A. R. obtained funding and directed the project.

Declaration of Competing Interest

The authors declare that they have no known competing financial interests or personal relationships that could have appeared to influence the work reported in this paper.

Data availability

Data will be made available on request.

Acknowledgement

This study was supported by the National Institutes of Health (R35 GM139572 to A. R.).

Appendix A. Supplementary data

Supplementary data to this article can be found online at https://doi.org/10.1016/j.bpc.2023.107092.

References

[1] T. Omura, R. Sato, A new cytochrome in liver microsomes, J. Biol. Chem. 237 (1962) 1375–1376.
[2] F.P. Guengerich, M.R. Waterman, M. Egli, Recent structural insights into cytochrome P450 function, Trends Pharmacol. Sci. 37 (2016) 625–640, https://doi.org/10.1016/j.tips.2016.05.006.
[3] F.P. Guengerich, Cytochrome P450 enzymes in the generation of commercial products, Nat. Rev. Drug Discov. 1 (2002) 359–366, https://doi.org/10.1038/nrd792.
[4] A.M. McDonnell, C.H. Dang, Basic review of the cytochrome P450 system, J. Adv. Pract. Oncol. 4 (2013) 263–268, https://doi.org/10.6004/jadpro.2013.4.4.7.
[5] U.H.N. Dürr, L. Waskell, A. Ramamoorthy, The cytochromes P450 and b5 and their reductases-promising targets for structural studies by advanced solid-state NMR spectroscopy, Biochim. Biophys. Acta Biomembr. 1768 (2007) 3235–3259, https://doi.org/10.1016/j.bbamem.2007.08.007.
[6] S.D. Black, Membrane topology of the mammalian P450 cytochromes, FASEB J. 6 (1992) 680–685, https://doi.org/10.1096/fasebj.6.2.1537456.
[7] F. Hannemann, A. Bichet, K.M. Ewen, R. Bernhardt, Cytochrome P450 systems-biological variations of electron transport chains, Biochim. Biophys. Acta Gen. Subj. 1770 (2007) 330–344, https://doi.org/10.1016/j.bbagen.2006.07.017.
[8] M.J.I. Paine, N.S. Scrutton, A.W. Munro, A. Gutierrez, G.C.K. Roberts, C. Roland Wolf, Electron transfer partners of cytochrome P450, in: Cytochrome P450: Structure, Mechanism, and Biochemistry, Third edition, 2005, pp. 115–148, https://doi.org/10.1007/0-387-27447-2_4.
[9] L. Waskell, J.J.P. Kim, Electron transfer partners of cytochrome P450, in: Cytochrome P450: Structure, Mechanism, and Biochemistry, Fourth edition, 2015, pp. 33–68, https://doi.org/10.1007/978-3-319-12108-6_2.
[10] J.B. Schenkman, I. Jansson, Interactions between cytochrome P450 and cytochrome b5, in, Drug Metab. Rev. (1999) 351–364, https://doi.org/10.1081/DMR-100101923.
[11] G. Vergères, L. Waskell, Cytochrome b5, its functions, structure and membrane topology, Biochimie. 77 (1995) 604–620, https://doi.org/10.1016/0300-9084(96)88176-4.
[12] J. Ozols, Structure of cytochrome b5 and its topology in the microsomal membrane, Biochim. Biophys. Acta (BBA)/Protein Struct. Mol. 997 (1989) 121–130, https://doi.org/10.1016/0167-4838(89)90143-X.
[13] M. Noshiro, V. Ullrich, T. Omura, Cytochrome b5 as Electron donor for oxy-cytochrome P-450, Eur. J. Biochem. 116 (1981) 521–526, https://doi.org/10.1111/j.1432-1033.1981.tb05367.x.
[14] M. Stiborová, R. Indra, M. Moserová, E. Frei, H.H. Schmeiser, K. Kopka, D. H. Philips, V.M. Arlt, NADH:cytochrome b5 reductase and cytochrome b5 can act as sole electron donors to human cytochrome P450 1A1-mediated oxidation and DNA adduct formation by Benzo[a]pyrene, Chem. Res. Toxicol. 29 (2016) 1325–1334, https://doi.org/10.1021/acs.chemrestox.6b00143.
[15] S.C. Im, L. Waskell, The interaction of microsomal cytochrome P450 2B4 with its redox partners, cytochrome P450 reductase and cytochrome b5, Arch. Biochem. Biophys. 507 (2011) 144–153, https://doi.org/10.1016/j.abb.2010.10.023.
[16] C.J. Henderson, L.A. McLaughlin, N. Scheer, L.A. Stanley, C.R. Wolf, Cytochrome b5 is a major determinant of human cytochrome P450 CYP2D6 and CYP3A4 activity in vivo, Mol. Pharmacol. 87 (2015) 733–739, https://doi.org/10.1124/mol.114.097394.
[17] J.B. Schenkman, I. Jansson, The many roles of cytochrome b5, Pharmacol. Ther. 97 (2003) 139–152, https://doi.org/10.1016/S0163-7258(02)00327-3.
[18] K.A. Gentry, M. Zhang, S.C. Im, L. Waskell, A. Ramamoorthy, Substrate mediated redox partner selectivity of cytochrome P450, chemical, Communication. 54 (2018) 5780–5783, https://doi.org/10.1039/c8cc02525h.
[19] K.A. Gentry, G.M. Anantharamaiah, A. Ramamoorthy, Probing protein-protein and protein-substrate interactions in the dynamic membrane-associated ternary complex of cytochromes P450, b_5, and reductase, chemical, Communication. 55 (2019) 13422–13425, https://doi.org/10.1039/c9cc05904k.
[20] J.W. Park, J.R. Reed, L.M. Brignac-Huber, W.L. Backes, Cytochrome P450 system proteins reside in different regions of the endoplasmic reticulum, Biochem. J. 464 (2014) 241–249, https://doi.org/10.1042/BJ20140787.
[21] M. Zhang, R. Huang, S.C. Im, L. Waskell, A. Ramamoorthy, Effects of membrane mimetics on cytochrome P450-cytochrome b5 interactions characterized by NMR spectroscopy, J. Biol. Chem. 290 (2015) 12705–12718, https://doi.org/10.1074/jbc.M114.597096.
[22] C. Barnaba, B.R. Sahoo, T. Ravula, I.G. Medina-Meza, S.C. Im, G. M. Anantharamaiah, L. Waskell, A. Ramamoorthy, Cytochrome-P450-induced ordering of microsomal membranes modulates affinity for drugs, Angew. Chem. Int. Ed. 57 (2018) 3391–3395, https://doi.org/10.1002/anie.201713167.
[23] B.C. Monk, T.M. Tomasiak, M.V. Keniya, F.U. Huschmann, J.D.A. Tyndall, J. D. O'Connell, R.D. Cannon, J.G. McDonald, A. Rodriguez, J.S. Finer-Moore, R. M. Stroud, Architecture of a single membrane spanning cytochrome P450 suggests constraints that orient the catalytic domain relative to a bilayer, Proc. Natl. Acad. Sci. U. S. A. 111 (2014) 3865–3870, https://doi.org/10.1073/pnas.1324245111.
[24] A.G. Bart, E.E. Scott, Structural and functional effects of cytochrome b5 interactions with human cytochrome P450 enzymes, J. Biol. Chem. 292 (2017) 20818–20833, https://doi.org/10.1074/jbc.RA117.000220.
[25] D.F. Estrada, A.L. Skinner, J.S. Laurence, E.E. Scott, Human cytochrome P450 17A1 conformational selection: modulation by ligand and cytochrome b5, J. Biol. Chem. 289 (2014) 14310–14320, https://doi.org/10.1074/jbc.M114.560144.
[26] H. Zhang, S.C. Im, L. Waskell, Cytochrome b5 increases the rate of product formation by cytochrome P450 2B4 and competes with cytochrome P450 reductase for a binding site on cytochrome P450 2B4, J. Biol. Chem. 282 (2007) 29766–29776, https://doi.org/10.1074/jbc.M703845200.
[27] M.B. Murataliev, V.M. Guzov, F.A. Walker, R. Feyereisen, P450 reductase and cytochrome b5 interactions with cytochrome P450: effects on house fly CYP6A1 catalysis, Insect Biochem. Mol. Biol. 38 (2008) 1008–1015, https://doi.org/10.1016/j.ibmb.2008.08.007.
[28] M. Zhang, R. Huang, R. Ackermann, S.C. Im, L. Waskell, A. Schwendeman, A. Ramamoorthy, Reconstitution of the Cytb5-CytP450 complex in nanodiscs for structural studies using NMR spectroscopy, Angew. Chem. Int. Ed. 55 (2016) 4497–4499, https://doi.org/10.1002/anie.201600073.
[29] K. Yamamoto, U.H.N. Dürr, J. Xu, S.C. Im, L. Waskell, A. Ramamoorthy, Dynamic interaction between membrane-bound full-length cytochrome P450 and cytochrome b5 observed by solid-state NMR spectroscopy, Sci. Rep. 3 (2013), https://doi.org/10.1038/srep02538.
[30] K. Yamamoto, M.A. Caporini, S.C. Im, L. Waskell, A. Ramamoorthy, Transmembrane interactions of full-length mammalian Bitopic cytochrome-P450-cytochrome-b 5 complex in lipid bilayers revealed by sensitivity-enhanced dynamic nuclear polarization solid-state NMR spectroscopy, Sci. Rep. 7 (2017), https://doi.org/10.1038/s41598-017-04219-1.
[31] K. Yamamoto, M. Gildenberg, S. Ahuja, S.C. Im, P. Pearcy, L. Waskell, A. Ramamoorthy, Probing the transmembrane structure and topology of microsomal cytochrome-P450 by solid-state NMR on temperature-resistant bicelles, Sci. Rep. 3 (2013) 2538, https://doi.org/10.1038/srep02556.
[32] U.H.N. Dürr, K. Yamamoto, S.C. Im, L. Waskell, A. Ramamoorthy, Solid-state NMR reveals structural and dynamical properties of a membrane-anchored electron-carrier protein, cytochrome b5, J. Am. Chem. Soc. 129 (2007) 6670–6671, https://doi.org/10.1021/ja069028m.
[33] N.M. Pearl, J. Wilcoxen, S. Im, R. Kunz, J. Darty, R.D. Britt, S.W. Ragsdale, L. Waskell, Protonation of the Hydroperoxo intermediate of cytochrome P450 2B4 is slower in the presence of cytochrome P450 reductase than in the presence of cytochrome b5, Biochemistry. 55 (2016) 6558–6567, https://doi.org/10.1021/acs.biochem.6b00996.
[34] V. Cojocaru, K. Balali-Mood, M.S.P. Sansom, R.C. Wade, Structure and dynamics of the membrane-bound cytochrome P450 2C9, PLoS Comput. Biol. 7 (2011), e1002152, https://doi.org/10.1371/journal.pcbi.1002152.
[35] G. Mustafa, P.P. Nandekar, X. Yu, R.C. Wade, On the application of the MARTINI coarse-grained model to immersion of a protein in a phospholipid bilayer, J. Chem. Phys. 143 (2015), 243139, https://doi.org/10.1063/1.4936909.
[36] Y.L. Cui, Q. Xue, Q.C. Zheng, J.L. Zhang, C.P. Kong, J.R. Fan, H.X. Zhang, Structural features and dynamic investigations of the membrane-bound cytochrome P450 17A1, Biochim. Biophys. Acta Biomembr. 2015 (1848) 2013–2021, https://doi.org/10.1016/j.bbamem.2015.05.017.
[37] N.A. Treuheit, M. Redhair, H. Kwon, W.D. McClary, M. Guttman, J.P. Sumida, W. M. Atkins, Membrane interactions, ligand-dependent dynamics, and stability of cytochrome P4503A4 in lipid Nanodiscs, Biochemistry. 55 (2016) 1058–1069, https://doi.org/10.1021/acs.biochem.5b01313.
[38] P. Jeřábek, J. Florián, V. Martínek, Membrane-anchored cytochrome P450 1A2-cytochrome b 5 complex features an X-shaped contact between antiparallel transmembrane helices, Chem. Res. Toxicol. 29 (2016) 626–636, https://doi.org/10.1021/acs.chemrestox.5b00349.
[39] Y. Zhang, I-TASSER server for protein 3D structure prediction, BMC Bioinform. 9 (2008) 40, https://doi.org/10.1186/1471-2105-9-40.
[40] N. Eswar, B. Webb, M.A. Marti-Renom, M.S. Madhusudhan, D. Eramian, M. Shen, U. Pieper, A. Sali, Comparative protein structure modeling using MODELLER, Curr. Protoc. Protein Sci. 50 (2007), https://doi.org/10.1002/0471140864.ps0209s50, 2.9.1-2.9.31.
[41] C. Dominguez, R. Boelens, A.M.J.J. Bonvin, HADDOCK: a protein-protein docking approach based on biochemical or biophysical information, J. Am. Chem. Soc. 125 (2003) 1731–1737, https://doi.org/10.1021/ja026939x.

[42] S. Ahuja, N. Jahr, S.C. Im, S. Vivekanandan, N. Popovych, S.V. Le Clair, R. Huang, R. Soong, J. Xu, K. Yamamoto, R.P. Nanga, A. Bridges, L. Waskell, A. Ramamoorthy, A model of the membrane-bound cytochrome b5-cytochrome P450 complex from NMR and mutagenesis data, J. Biol. Chem. 288 (2013) 22080–22095, https://doi.org/10.1074/jbc.M112.448225.

[43] S. Jo, T. Kim, V.G. Iyer, W. Im, CHARMM-GUI: a web-based graphical user interface for CHARMM, J. Comput. Chem. 29 (2008) 1859–1865, https://doi.org/10.1002/jcc.20945.

[44] J. Huang, A.D. Mackerell, CHARMM36 all-atom additive protein force field: validation based on comparison to NMR data, J. Comput. Chem. 34 (2013) 2135–2145, https://doi.org/10.1002/jcc.23354.

[45] B.R. Sahoo, T. Fujiwara, Conformational states of HAMP domains interacting with sensory rhodopsin membrane systems: an integrated all-atom and coarse-grained molecular dynamics simulation approach, Mol. BioSyst. 13 (2017) 193–207, https://doi.org/10.1039/c6mb00730a.

[46] E.F. Pettersen, T.D. Goddard, C.C. Huang, G.S. Couch, D.M. Greenblatt, E.C. Meng, T.E. Ferrin, UCSF chimera - a visualization system for exploratory research and analysis, J. Comput. Chem. 25 (2004) 1605–1612, https://doi.org/10.1002/jcc.20084.

[47] R.A. Laskowski, M.B. Swindells, LigPlot+: multiple ligand-protein interaction diagrams for drug discovery, J. Chem. Inf. Model. 51 (2011) 2778–2786, https://doi.org/10.1021/ci200227u.

[48] S.J. Marrink, H.J. Risselada, S. Yefimov, D.P. Tieleman, A.H. De Vries, The MARTINI force field: coarse grained model for biomolecular simulations, J. Phys. Chem. B 111 (2007) 7812–7824, https://doi.org/10.1021/jp071097f.

[49] B.R. Sahoo, J. Maharana, M.C. Patra, G.K. Bhoi, S.K. Lenka, P.K. Dubey, S. Goyal, B. Dehury, S.K. Pradhan, Structural and dynamic investigation of bovine folate receptor alpha (FOLR1), and role of ultra-high temperature processing on conformational and thermodynamic characteristics of fOLR1-folate complex, Colloids Surf. B: Biointerfaces 121 (2014) 307–318, https://doi.org/10.1016/j.colsurfb.2014.05.028.

[50] J.M.J. Swanson, R.H. Henchman, J.A. McCammon, Revisiting free energy calculations: a theoretical connection to MM/PBSA and direct calculation of the association free energy, Biophys. J. 86 (2004) 67–74, https://doi.org/10.1016/S0006-3495(04)74084-9.

[51] C. Paissoni, D. Spiliotopoulos, G. Musco, A. Spitaleri, GMXPBSA 2.1: a GROMACS tool to perform MM/PBSA and computational alanine scanning, Comput. Phys. Commun. 186 (2015) 105–107, https://doi.org/10.1016/j.cpc.2014.09.010.

[52] B.R. Sahoo, J. Maharana, G.K. Bhoi, S.K. Lenka, M.C. Patra, M.R. Dikhit, P. K. Dubey, S.K. Pradhan, B.K. Behera, A conformational analysis of mouse Nalp3 domain structures by molecular dynamics simulations, and binding site analysis, Mol. BioSyst. 10 (2014) 1104–1116, https://doi.org/10.1039/c3mb70600a.

[53] B.R. Sahoo, T. Genjo, K.C. Moharana, A. Ramamoorthy, Self-assembly of polymer-encased lipid Nanodiscs and membrane protein reconstitution, J. Phys. Chem. B 123 (2019) 4562–4570, https://doi.org/10.1021/acs.jpcb.9b03681.

[54] N. Kučerka, M.P. Nieh, J. Katsaras, Fluid phase lipid areas and bilayer thicknesses of commonly used phosphatidylcholines as a function of temperature, Biochim. Biophys. Acta Biomembr. 2011 (1808) 2761–2771, https://doi.org/10.1016/j.bbamem.2011.07.022.

[55] K. Yamamoto, M.A. Caporini, S.C. Im, L. Waskell, A. Ramamoorthy, Transmembrane interactions of full-length mammalian Bitopic cytochrome-P450-cytochrome-b 5 complex in lipid bilayers revealed by sensitivity-enhanced dynamic nuclear polarization solid-state NMR spectroscopy, Sci. Rep. 7 (2017) 4116, https://doi.org/10.1038/s41598-017-04219-1.

[56] G. Mustafa, P.P. Nandekar, T.J. Camp, N.J. Bruce, M.C. Gregory, S.G. Sligar, R. C. Wade, Influence of transmembrane Helix mutations on cytochrome P450-membrane interactions and function, Biophys. J. 116 (2019) 419–432, https://doi.org/10.1016/j.bpj.2018.12.014.

[57] A. Bridges, L. Gruenke, Y.T. Chang, I.A. Vakser, G. Loew, L. Waskell, Identification of the binding site on cytochrome P450 2B4 for cytochrome b5 and cytochrome P450 reductase, J. Biol. Chem. 273 (1998) 17036–17049, https://doi.org/10.1074/jbc.273.27.17036.

[58] G. Mustafa, P.P. Nandekar, G. Mukherjee, N.J. Bruce, R.C. Wade, The effect of force-field parameters on cytochrome P450-membrane interactions: structure and dynamics, Sci. Rep. 10 (2020) 7284, https://doi.org/10.1038/s41598-020-64129-7.

[59] M. Zhang, S.V. Le Clair, R. Huang, S. Ahuja, S.C. Im, L. Waskell, A. Ramamoorthy, Insights into the role of substrates on the interaction between cytochrome b5 and cytochrome P450 2B4 by NMR, Sci. Rep. 5 (2014) 8392, https://doi.org/10.1038/srep08392.

[60] D.F. Estrada, J.S. Laurence, E.E. Scott, Substrate-modulated cytochrome P450 17A1 and cytochrome b5 interactions revealed by NMR, J. Biol. Chem. 288 (2013) 17008–17018, https://doi.org/10.1074/jbc.M113.468926.

[61] H. Hong, T.M. Blois, Z. Cao, J.U. Bowie, Method to measure strong protein-protein interactions in lipid bilayers using a steric trap, Proc. Natl. Acad. Sci. U. S. A. 107 (2010) 19802–19807, https://doi.org/10.1073/pnas.1010348107.

[62] J. Kriegsmann, M. Brehs, J.P. Klare, M. Engelhard, J. Fitter, Sensory rhodopsin II/transducer complex formation in detergent and in lipid bilayers studied with FRET, Biochim. Biophys. Acta Biomembr. 1788 (2009) 522–531, https://doi.org/10.1016/j.bbamem.2008.11.011.

[63] D. Flöck, V. Helms, A Brownian dynamics study: the effect of a membrane environment on an electron transfer system, Biophys. J. 87 (2004) 65–74, https://doi.org/10.1529/biophysj.103.035261.